Asociación Argentina
de Mecánica Computacional

Mecánica Computacional Vol XXX, págs. 1561-1574 (artículo completo)
Oscar Möller, Javier W. Signorelli, Mario A. Storti (Eds.)
Rosario, Argentina, 1-4 Noviembre 2011

EFFECT OF TEMPERATURE-DEPENDENT VISCOSITY ON THE FINAL SHEET THICKNESS IN THE CALENDERING OF NEWTONIAN SHEETS OF FINITE THICKNESS

José C. Arcos[a], 0scar E. Bautista[a], Federico Méndez[b] and Eric G. Bautista[a]

[a]*ESIME Azcapotzalco, Instituto Politécnico Nacional, Av. de las Granjas No. 682, Col. Santa Catarina, Del. Azcapotzalco, México, D.F. 02250, México. jarcos@ipn.mx,*
http://www.sepi.esimeazc.ipn.mx/mctf.html

[b]*Departamento de Termofluidos, Facultad de Ingeniería, UNAM, México, D.F. 04510, México.*
http://ingenieria.posgrado.unam.mx/mecanica/index.html

Keywords: Non-isothermal, Exiting Sheet Thickness, Crank-Nicolson Method.

Abstract. In this work, a non-isothermal simplified model for the calendering process of a Newtonian liquid with exponential dependence of viscosity on temperature is theoretically treated. The effects of non-isothermal conditions on the exiting sheet thickness in calendering process are investigated. The mass, momentum and energy balance equations, based on the lubrication theory, were nondimensionalized and solved for the velocity, pressure and temperature fields by using perturbation and numerical techniques, where the leave-off distance of the calendered material is unknown and represents an eigenvalue of the mathematical problem. With the knowledgement of the above variables, the exiting sheet thickness in the calendering process was determined. The mentioned governing equations contain basically two dimensionless parameters: the well-known Graetz number, Gz; and a parameter that takes into account the effect of the variable viscosity as a function of the temperature, defined as the ratio of the Nahme-Griffith number, Na, to the Graetz number, Gz. For values of this parameter much less than unity, the dimensionless exiting sheet thickness of the calendering process has been obtained as a function of the involved dimensionless parameters. The numerical results show that the inclusion of temperature-dependent viscosity effect reduces about 6 % the dimensionless exiting sheet thickness, or 20 % in the leave-off distance in comparison with the case of temperature independent viscosity.

Symbol Definition

a	empirical parameter
c_p	heat capacity [J/kg K]
Gz	Graetz number
$h(\bar{x})$	distance from center plane to periphery of roll at any value of $\bar{x}$
H_0	one-half of the thickness at the nip [m]
H_f	one-half of the incoming sheet thickness [m]
H	one-half of the exiting sheet thickness [m]
μ_0	reference consistency index [Pa s]
Na	Nahme-Griffith number
P	dimensionless pressure
$\bar{P}$	pressure in physical units [Pa]
Pe	Peclet number
$\bar{Q}$	flow rate, in physical units [m^3/s]
Q	dimensionless flow rate
R	cylinder radius [m]
Re	modified Reynolds number
T	temperature [K]
T_0	reference temperature [K]
ΔT_c	characteristic temperature rise [K]
u, v	dimensionless longitudinal and transversal velocities
U	roll speed [m/s]
$\bar{u}, \bar{v}$	longitudinal and transversal velocities in physical units [m/s]
$\bar{x}, \bar{y}$	cartesian coordinates
Y	dimensionless transversal coordinate, $Y = y/(1+\chi^2)$

Greek Letters

β	aspect ratio, defined as $\beta = \sqrt{H_0/2R}$
ϵ	dimensionless parameter, defined as $\epsilon = Na/Gz$
η	non-newtonian viscosity
θ	dimensionless temperature of the fluid
θ_0	dimensionless temperature zeroth-order, ϵ^0
θ_1	dimensionless temperature first order, ϵ^1
λ	leave-off distance
λ_0	leave-off distance zeroth-order
λ_1	leave-off distance first-order
ρ	fluid density [kg/m^3]
τ	dimensionless shear stress
$\bar{\tau}_{xy}$	shear stress in physical units [Pa]
χ	dimensionless longitudinal coordinate
ω	angular velocity

1 INTRODUCTION

The viscous fluid flow through the narrow region between two rotating rolls in such a way as to produce a thin sheet has been extensively studied over the past 50 years. The theoretical analysis regarding the above mechanism was developed by Gaskell (1950) and Mckelvey (1962) for a isothermal Newtonian fluid. Zheng and Tanner (1988) carried out an analysis of the calendering process using the power-law and the Phan-Thien-Tanner fluid models. For the viscoelastic case, they determined the separation point using the criterion of zero tangential traction. As a results they determined that unlike the inelastic case, the sheet was found to thicken after leaving the nip. Sofou and Mitsoulis (2004) used the lubrication approximation theory to provide numerical results for isothermal viscoplastic calendering sheets with a desired final thickness. Mitsoulis (2008) numerically investigated the shape of the free surfaces of the entering and exiting sheets for the process of calendering viscoplastic sheets with a finite thickness. The combined effects of asymmetry and viscous heating for the non-isothermal nip flow in calendering were considered by Dobbels and Mewis (1977). The effect of viscous dissipation on calendering process of Newtonian and power-law fluids have been studied by C. Kiparissides (1978). They reported the temperature profiles due to viscous dissipation in calendering gap, finding two maxima in the vicinity of the roll surfaces. In this context, Middleman (1977) developed a simple model of the sensitivity of calendered thickness to temperature fluctuations. He concluded that "*a 3° variation in temperature will cause more than 20 % variation in calendered thickness!*". In this sense, to our knowledge there are no works that validate the aforementioned sentence. Therefore, the goal of this work is to determine the influence of temperature-dependent viscosity on the exiting sheet thickness.

2 FORMULATION

In Fig. 1, we show the sketch of the studied physical model. Two cylinders separated by a thin film of a Newtonian liquid with temperature dependent viscosity, are rotated in the same direction. Each cylinder has a radius R, rotating with a constant angular velocity, ω, resulting in a linear velocity at its surface given by $U = \omega R$. The minimum gap half-height, H_0, is such that $H_0 \ll R$ and the one-half exiting sheet thickness is represented by H. The geometry of the roll surface is given as $h(\overline{x}) = H_0\left(1 + \overline{x}^2/2RH_0\right)$ Middleman (1977). The roll surfaces are found at a constant temperature, T_0. The location $\overline{x}$ where the sheet first bites the rolls is represented by $-\overline{x}_f$, which is known. On the other hand, the leave-off distance location of the sheet, modified by temperature effects, represented by λ is unknown, and must be determined in the present analysis. Due to the symmetry of the physical model, we consider only for convenience, the upper half of this configuration. The axis $\overline{y}$ points up, i.e., in the opposite direction of the gravity vector, and the positive $\overline{x}$ axial axis points in the direction of the flow as is shown in Fig. 1.

The mass, momentum and energy equations, in steady state, are the following

$$\frac{\partial \overline{u}}{\partial \overline{x}} + \frac{\partial \overline{v}}{\partial \overline{y}} = 0 \quad , \tag{1}$$

$$\rho\overline{u}\frac{\partial \overline{u}}{\partial \overline{x}} + \rho\overline{v}\frac{\partial \overline{u}}{\partial \overline{y}} = -\frac{\partial \overline{P}}{\partial \overline{x}} + \frac{\partial \overline{\tau}_{yx}}{\partial \overline{y}} \quad , \tag{2}$$

$$\rho\overline{u}\frac{\partial \overline{v}}{\partial \overline{x}} + \rho\overline{v}\frac{\partial \overline{v}}{\partial \overline{y}} = -\frac{\partial \overline{P}}{\partial \overline{y}} + \frac{\partial \overline{\tau}_{xy}}{\partial \overline{x}} \quad , \tag{3}$$

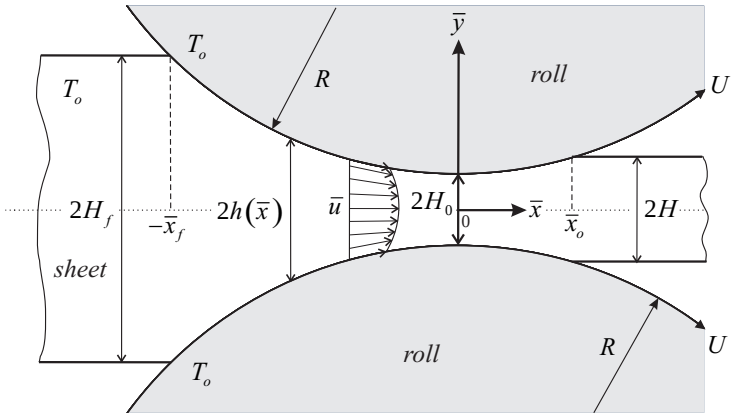

Figure 1: Schematic diagram of the studied physical model, in physical variables.

$$\rho c_p \overline{u} \frac{\partial T}{\partial \overline{x}} = k \left(\frac{\partial^2 T}{\partial \overline{x}^2} + \frac{\partial^2 T}{\partial \overline{y}^2} \right) + \overline{\tau}_{xy} \frac{\partial \overline{u}}{\partial \overline{y}} \quad ; \tag{4}$$

where the shear stress is given as Tadmor and Gogos (1979),

$$\overline{\tau}_{xy} = \mu_0 \exp\left[-a\left(T - T_0\right)\right] \left(\frac{\partial \overline{u}}{\partial \overline{y}} + \frac{\partial \overline{v}}{\partial \overline{x}} \right) \quad . \tag{5}$$

The boundary and initial conditions associated with Eqs. (1)-(4) are

$$\overline{y} = 0 : \frac{\partial \overline{u}}{\partial \overline{y}} = 0 \quad , \tag{6}$$

$$\overline{y} = h\left(\overline{x}\right) : \overline{u} = U \quad , \tag{7}$$

$$\overline{y} = 0 : \frac{\partial T}{\partial \overline{y}} = 0 \quad , \tag{8}$$

$$\overline{y} = h\left(\overline{x}\right) : T = T_0 \quad , \tag{9}$$

$$\overline{x} = -\overline{x}_f : T = T_0 \quad . \tag{10}$$

The boundary conditions (6-10) are those used in the lubrication approximation theory. In the above equations, $\overline{u}$, $\overline{v}$, $\overline{P}$ and T represent the velocity components in $\overline{x}$ and $\overline{y}$ directions, pressure and temperature fields of the fluid, respectively. ρ, c_p, k, μ_0 are the density, heat capacity, thermal conductivity and the viscosity of the Newtonian liquid evaluated at a reference temperature T_0, respectively. In addition, a is an empirical parameter that measures the dependence of the viscosity on the temperature; this constant is of order of 10^{-2} to 10^{-1} Dobbels and Mewis (1977); Dantzig and Tucker (2001). In Eq. (5) we have included the exponential temperature dependence model for the viscosity Dantzig and Tucker (2001). We can identify the following scales for $\overline{x}$, $\overline{y}$ and $\overline{u}$

$$\overline{x} \sim \sqrt{2RH_0} \; , \; \overline{y} \sim H_0 \; , \; \overline{u} \sim U \quad , \tag{11}$$

from the mass conservation equation, Eq. (1), and taking into account the relationships (11) , we obtain

$$\frac{\overline{v}_c}{U} \sim \frac{H_0}{L_c} \ll 1, \tag{12}$$

indicating that the order of magnitude of the transversal velocity, $\overline{v}_c$, is smaller than the longitudinal velocity. For obtaining the characteristic temperature rise, we compare the convective and viscous dissipation terms in the energy equation, Eq. (4), yielding

$$\Delta T_c \sim \sqrt{\frac{2R}{H_0}} \frac{\mu_0}{\rho_f c_p} \frac{U}{H_0} \quad . \tag{13}$$

The previous characteristic scales will be used to nondimensionalize the governing equations properly.

2.1 Dimensionless equations

In this section, we present the dimensionless governing equations needed to solve the non-isothermal calendering process (Fig. 2). Based on the order of magnitude analysis carried out previously, we define the following dimensionless variables

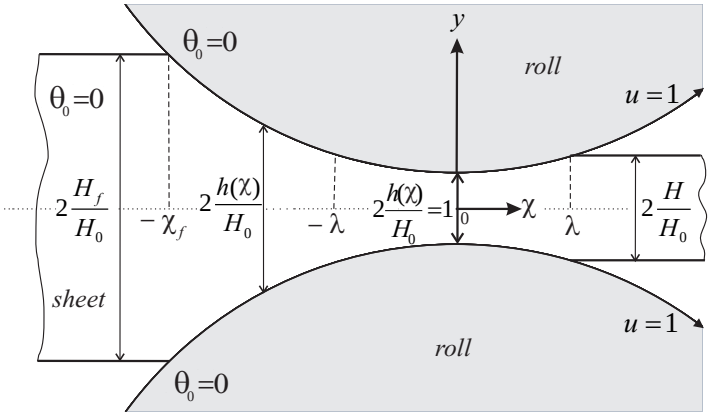

Figure 2: Schematic diagram of the studied physical model, in dimensionless variables.

$$\begin{aligned} \chi &= \frac{\overline{x}}{\sqrt{2RH_0}}, \quad y = \frac{\overline{y}}{H_0}, \quad \frac{h\left(\overline{x}\right)}{H_0} = 1 + \chi^2 \\ P &= \frac{\overline{P}H_0}{\mu_0 U}, \quad \lambda^2 = \frac{H}{H_0} - 1, \quad Q\left(\chi\right) = \frac{\overline{Q}}{2UH_0} \\ u\left(\chi, y\right) &= \frac{\overline{u}\left(\overline{x}, \overline{y}\right)}{U}, v\left(\chi, y\right) = \frac{\overline{v}\left(\overline{x}, \overline{y}\right)}{v_c}, \theta\left(\chi, y\right) = \frac{T\left(\overline{x}, \overline{y}\right) - T_0}{\Delta T_c}. \end{aligned} \tag{14}$$

Introducing the dimensionless variables defined by relationships (14) into the conservation equations (1)-(5), we obtain

$$Re\beta \left(u\frac{\partial u}{\partial \chi} + v\frac{\partial u}{\partial y} \right) = -\beta \frac{dP}{d\chi} + \frac{\partial}{\partial y}\left(e^{-\epsilon\theta} \frac{\partial u}{\partial y} \right), \tag{15}$$

$$Gz\, u\frac{\partial\theta}{\partial\chi} = \frac{\partial^2\theta}{\partial y^2} + Gz\, e^{-\epsilon\theta}\left(\frac{\partial u}{\partial y}\right)^2 \quad . \tag{16}$$

Here, ϵ is a dimensionless parameter, given as $\epsilon = Na/Gz$, where Na is the Nahme-Griffith number Dantzig and Tucker (2001); Osswald and Ortiz (2006); Bird et al. (1987), defined as $Na = a\,(\mu_0 U^2/k)$, and Gz is the well known Graetz number, given by $Gz = \beta Pe$. Here Pe is the Peclet number, represented by $Pe = (\rho c_p/k)\,UH_0$, and β is a geometric parameter, defined as $\beta = (H_0/2R)^{1/2}$. The Nahme-Griffith number represents the ratio of the temperature rise, due to viscous dissipation to the temperature rise needed to change the viscosity. Re is the Reynolds number, defined as $Re = \rho U H_0/\mu_0$. In typical applications of calendering, $\epsilon \ll 1$, in such a way that the exponential factor, in the momentum and energy equations, can be linearized as $e^{-\epsilon\theta} \approx 1 - \epsilon\theta + \cdots$, and the Reynolds number is much less than unity, $Re \sim 10^{-4} - 10^{-5}$, indicating that the inertia plays a minor role in this process; the Peclet number takes values of order of 10^2 to 10^3. According to the previous discussion, Eq. (15) transforms to

$$\beta\frac{dP}{d\chi} = \frac{\partial}{\partial y}\left[(1 - \epsilon\theta + \cdots)\,\frac{\partial u}{\partial y}\right] \quad , \tag{17}$$

with the following dimensionless boundary conditions,

$$\left.\frac{\partial u}{\partial y}\right|_{y=0} = 0 \quad , \tag{18}$$

$$u\left(y = 1 + \chi^2\right) = 1 \quad . \tag{19}$$

Furthermore, Eq. (17) requires the boundary conditions for the pressure gradient $dP/d\chi$ and the pressure P, given by

$$\left.\frac{dP}{d\chi}\right|_{\chi=\lambda} = P\,(\chi = \lambda) = 0 \quad , \tag{20}$$

$$P\,(\chi = -\chi_f) = 0 \quad . \tag{21}$$

The energy equation, Eq. (16), takes the form

$$Gz\, u\frac{\partial\theta}{\partial\chi} = \frac{\partial^2\theta}{\partial y^2} + Gz\ (1 - \epsilon\theta + \cdots)\left(\frac{\partial u}{\partial y}\right)^2 \quad , \tag{22}$$

with the boundary conditions,

$$\theta\,(-\chi_f, y) = 0 \quad , \tag{23}$$

$$\theta\left(\chi, 1 + \chi^2\right) = 0 \quad , \tag{24}$$

$$\left.\frac{\partial\theta}{\partial y}\right|_{y=0} = 0 \quad . \tag{25}$$

Together with Eqs. (17) and (22), we need the dimensionless mass balance equation, which can be written in the form,

$$Q = 1 + \lambda^2 = \int_0^{1+\chi^2} u \, dy \quad , \tag{26}$$

where Q, for the present formulation, assumes a constant value and represents the volumetric flow rate; λ represents an eigenvalue of the mathematical problem, to be obtained, which is related to the exiting sheet thickness in the calendering process by the following relationship $\lambda^2 = H/H_0 - 1$. This parameter will be influenced by temperature effects in contrast to those that not consider thermal aspects. The system of equations (17) and (22) represent the well known *lubrication approximation* Pearson (1966) for a Newtonian liquid with temperature-dependent viscosity.

3 ASYMPTOTIC SOLUTION FOR THE LIMIT $\epsilon \ll 1$.

To determine the dimensionless velocity, pressure, temperature profiles, leave-off distance and the corresponding exiting thickness of the calendered material, we conduct an asymptotic solution for decoupling the system of Eqs. (17) and (22). Applying a regular perturbation technique and using ϵ as the perturbation parameter, we propose the following expansions,

$$u(\chi, y) = u_0(\chi, y) + \epsilon u_1(\chi, y) + \cdots \quad , \tag{27}$$

$$P(\chi) = P_0(\chi) + \epsilon P_1(\chi) + \cdots \quad , \tag{28}$$

$$Q = Q_0 + \epsilon Q_1 + \cdots \quad , \tag{29}$$

$$\theta(\chi, y) = \theta_0(\chi, y) + \epsilon \theta_1(\chi, y) + \cdots \quad , \tag{30}$$

$$\lambda = \lambda_0 + \epsilon \lambda_1 + \cdots \quad , \tag{31}$$

where u_0, P_0, Q_0, λ_0 and θ_0 are the leading-order solutions, which represent the isothermal case and solved in previous works Sofou and Mitsoulis (2004); Middleman (1977). P_1, Q_1, u_1, θ_1 and λ_1 are corrections up to first-order terms. Introducing the relationships (27)-(31) into Eqs. (17)-(26), we obtain, after collecting terms of the same power of ϵ, the following sets of equations

for ϵ^0 :

$$\beta \frac{dP_0}{d\chi} = \frac{\partial^2 u_0}{\partial y^2}, \quad \text{for} \quad -\chi_f \leq \chi \leq \lambda_0 \quad , \tag{32}$$

$$Q_0 = 1 + \lambda_0^2 = \int_0^{1+\chi^2} u_0 dy \quad , \tag{33}$$

$$Gz \; u_0 \frac{\partial \theta_0}{\partial \chi} = \frac{\partial^2 \theta_0}{\partial y^2} + Gz \left(\frac{\partial u_0}{\partial y} \right)^2 \quad . \tag{34}$$

The boundary conditions for Eqs. (32)-(34) are:

$$\frac{\partial u_0}{\partial y} = 0 \quad \text{and} \quad \frac{\partial \theta_0}{\partial y} = 0, \quad \text{at} \quad y = 0, \tag{35}$$

$$u_0 = 1 \quad \text{and} \quad \theta_0 = 0, \quad \text{at} \quad y = 1 + \chi^2, \tag{36}$$

$$P_0 = 0 \quad \text{and} \quad \theta_0 = 0, \quad \text{at} \quad \chi = -\chi_f, \tag{37}$$

$$\frac{dP_0}{d\chi} = P_0 = 0 \quad \text{at} \quad \chi = \lambda_0. \tag{38}$$

For the first order solution, ϵ^1 :

$$\beta \frac{dP_1}{d\chi} y = \frac{\partial u_1}{\partial y} - \theta_0 \frac{\partial u_0}{\partial y}, \text{for } -\chi_f \leq \chi \leq \lambda_1 \quad , \tag{39}$$

$$Q_1 = 2\lambda_0 \lambda_1 = \int_0^{1+\chi^2} u_1 dy \quad . \tag{40}$$

For solving Eqs. (39) and (40), we need the zeroth-order solution for mass, momentum and energy equations, Eqs. (32)-(34). The boundary conditions for Eqs. (39) and (40) are written as,

$$\frac{\partial u_1}{\partial y} = 0 \quad \text{and} \quad \frac{\partial \theta_1}{\partial y} = 0, \quad \text{at} \quad y = 0, \tag{41}$$

$$u_1 = 0 \quad \text{and} \quad \theta_1 = 0, \quad \text{at} \quad y = 1 + \chi^2, \tag{42}$$

$$P_1 = 0 \quad \text{and} \quad \theta_1 = 0, \quad \text{at} \quad \chi = -\chi_f, \tag{43}$$

$$\frac{dP_1}{d\chi} = P_1 = 0 \quad \text{at} \quad \chi = \lambda_1. \tag{44}$$

3.1 Zeroth-order solution

The solution of Eq.(32), considering a finite feed thickness, is given by:

$$u_0 = 1 + \frac{1}{2}\beta \left(\frac{dP_0}{d\chi} \right) \left[y^2 - \left(1 + \chi^2\right)^2 \right], \tag{45}$$

with

$$\frac{dP_0}{d\chi} = -3\beta^{-1} \frac{(\lambda_0^2 - \chi^2)}{(1 + \chi^2)^3} \quad , \tag{46}$$

for $-\chi_f \leq \chi \leq \lambda_0$.

We must emphasize that the zeroth-order solution, Eqs. (45) and (46), were obtained in previous works Gaskell (1950); Sofou and Mitsoulis (2004). In the present analysis, the zeroth-order energy equation, Eq. (34), was solved in the two flow regions in the χ direction: one region

near to the nip at the entrance to the rolls, which has a positive pressure gradient; and the other region away from the nip at the exit, with opposite sign for the pressure gradient.

Due to the curvature of the rolls, we use a simple independent variable transformation that makes possible to solve the dimensionless energy equation on a uniformly spaced computational grid, therefore we can introduce the following transformation variable, $Y = y/\left(1+\chi^2\right)$ Wendt (2009), then Eq. (34) takes the form,

$$Gz\, u_0 \frac{\partial \theta_0}{\partial \chi} = \frac{1}{\left(1+\chi^2\right)^2}\frac{\partial^2 \theta_0}{\partial Y^2} + Gz\left(\frac{1}{1+\chi^2}\frac{\partial u_0}{\partial Y}\right)^2 \quad . \tag{47}$$

In the new independent variable, Y, the zeroth-order velocity profile is given by

$$u_0 = 1 + \frac{3}{2}\frac{\left(\chi^2-\lambda_0^2\right)}{1+\chi^2}\left(Y^2-1\right) \quad , \tag{48}$$

the boundary conditions, given by Eqs. (35) and (36), associated with the Eq. (47) are transformed to

$$Y = 0 : \frac{\partial \theta_0}{\partial Y} = 0 \quad , \tag{49}$$

$$Y = 1 : \theta_0 = 0 \quad . \tag{50}$$

Equation (47) was numerically solved by using a the conventional Crank-Nicolson method Hoffman (2001). To solve this equation, we selected a mesh with 501 nodal points for the half width and 1027 in the direction of the flow. The details are omitted for simplicity.

3.2 First order solution

The solution procedure for the first-order is similar to the zeroth-order solution; the Eq. (39) is integrated to find u_1 explicitly as a function of Y, and implicitly as a function of $dP_1/d\chi$. In terms of the the independent variable transformation $y = \left(1+\chi^2\right)Y$, after applying the boundary conditions (41) and (42) takes the form,

$$u_1\left(\chi, Y\right) = \frac{1}{2}\beta\left(1+\chi^2\right)^2\frac{dP_1}{d\chi}\left[Y^2-1\right] - \beta\left(1+\chi^2\right)^2\frac{dP_0}{d\chi}\left[\int_0^1 \theta_0 Y dY - \int_0^Y \theta_0 Y dY\right] \quad . \tag{51}$$

Replacing Eq. (51) into Eq. (40), gives the volumetric flow rate for the first order,

$$Q_1 = -\beta\frac{\left(1+\chi^2\right)^3}{3}\frac{dP_1}{d\chi} - \beta\left(1+\chi^2\right)^3\left(\frac{dP_0}{d\chi}\right)\left[\int_0^1\int_0^1 \theta_0 Y dY dY - \int_0^1\int_0^Y \theta_0 Y dY dY\right] \quad , \tag{52}$$

where $dP_0/d\chi$ in Eqs. (51)-(52) is defined by Eq. (46). Apply the boundary condition, given by Eq. (44), into Eq. (52), and after some algebraic manipulation, we can obtain one explicit expression for $dP_1/d\chi$

$$\frac{dP_1}{d\chi} = 9\beta^{-1}\left\{\begin{array}{c} \frac{\left(\lambda_0^2-\chi^2\right)}{\left(1+\chi^2\right)^3}\left[\int_0^1\int_0^1 \theta_0 Y dY dY - \int_0^1\int_0^Y \theta_0 Y dY dY\right] \\ -\frac{\left(\lambda_0^2-\lambda_1^2\right)}{\left(1+\chi^2\right)^3}\left[\int_0^1\int_0^1 \theta_0 Y dY dY - \int_0^1\int_0^Y \theta_0 Y dY dY\right]_{\chi=\lambda_1} \end{array}\right\} \tag{53}$$

This equation is valid for $-\chi_f \leq \chi \leq \lambda_1$, where λ_1 must be determined as a part of the problem. In the above equation, the procedure to evaluate the integral terms is the following: at each axial position , χ, the term given by the first integral, $\int_0^1 \int_0^1 \theta_0 Y dY \; dY$, is found numerically by using the Trapezoidal rule Hoffman (2001). Specifically, this procedure was implemented at each axial position, χ, from the point where the entering sheet first bites the rolls Middleman (1977) to the leave-off distance point of the rolls, given by the zeroth order solution of λ_0. For the obtained data in this numerical integration, one ninth-degree polynomial regression was generated as a function of the coordinate axial χ. In order to find the first order of the dimensionless flow rate, Q_1, and consequently λ_1, an iterative procedure was applied to Eq. (53).

Table 1: Representative values of kinematic parameters and physical properties of Newtonian liquids.

U	0.25 - 0.09 m/s
H_0	0.0001 - 0.0010 m
R	0.20 - 0.50 m
a	0.01 - 0.1 K^{-1}
k	0.13 - 0.16 W/m K
μ_0	1000 Pa-s
c_p	1716 - 2100 J/kg K
ρ	1000 kg/m^3

4 RESULTS AND DISCUSSION

For the numerical results presented in this section, we used representative values of the parameters involved in the calendering process (see Table 1)Dobbels and Mewis (1977); C. Kiparissides (1978). Figures 3 and 4 show the numerical solution for the dimensionless temperature θ_0 as a function of the dimensionless transverse direction at five axial positions, χ, for two fixed different entering sheet thickness, H_f/H_0(=1.543, 3.337) and Gz=40, respectively. In these figures, we note that the maximum values of the dimensionless temperature are confined to the vicinity of the roll surface for each χ position, these are the results of the interaction between the viscous dissipation of the fluid and the heat transfer mechanisms to the rolls. For the same figures, the larger values of the dimensionless temperature in the χ direction are located near to the entry. Specifically, in these figures the maximum dimensionless temperature are located at $\chi = -0.432$ and $\chi = -0.623$, respectively. In addition, it can be seen that for increasing values of H_f/H_0, the dimensionless temperature θ_0, is increased.

In Fig. 5, we present the dimensionless pressure up terms or order ϵ, $P = P_0 + \epsilon P_1 + \cdots$, for different values of the parameter ϵ. In all cases, for increasing values of the parameter ϵ, insignificantly changes in the dimensionless pressure field are appreciated. However,as a direct consequence of the temperature variation in the process, the value of λ for which the fluid leaves off the rolls (and compared with the isothermal case), is modified. This variation in λ is because we have considered a correction due to the effects of the temperature-dependent viscosity of the fluid. As we can see, in Fig. 6 we show the influence of the parameter ϵ on the exiting sheet thickness: for increasing values of this parameter, the dimensionless axial pressure vanishes at a position located before that predicted for the isothermal case.

In Figs. 7 we present the complete results for the dimensionless exiting sheet thickness

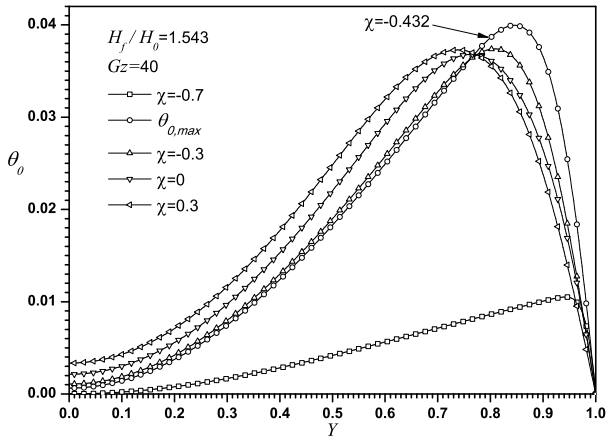

Figure 3: Dimensionless temperature θ_0 as a function of the dimensionless longitudinal χ and transversal Y coordinates, $Gz = 40$, H_f/H_0 =1.543, at five different positions of the variable χ

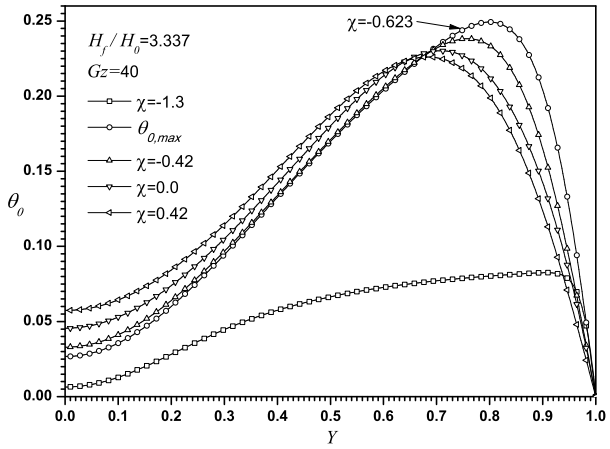

Figure 4: Dimensionless temperature θ_0 as a function of the dimensionless longitudinal χ and transversal Y coordinates, $Gz = 40$, H_f/H_0 =3.337, at five different positions of the variable χ

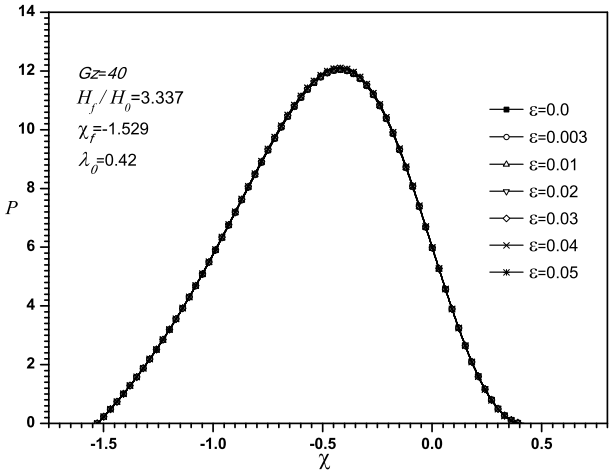

Figure 5: Dimensionless pressure profiles in the gap, along the flow field for different values of the parameter ϵ, $Gz = 40$, H_f/H_0=3.337

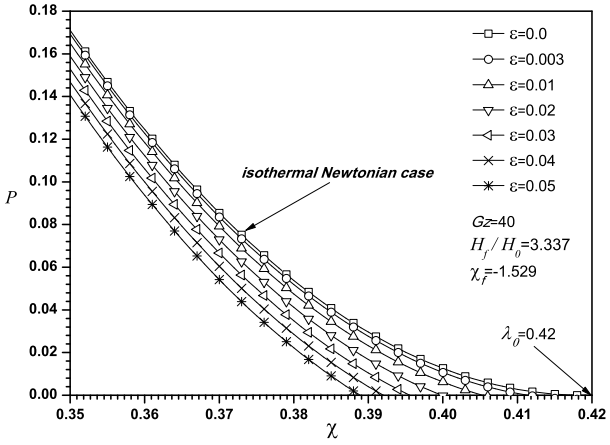

Figure 6: Dimensionless pressure profiles in the gap, along the flow field for different values of the parameter ϵ, $Gz = 40$, H_f/H_0=3.337

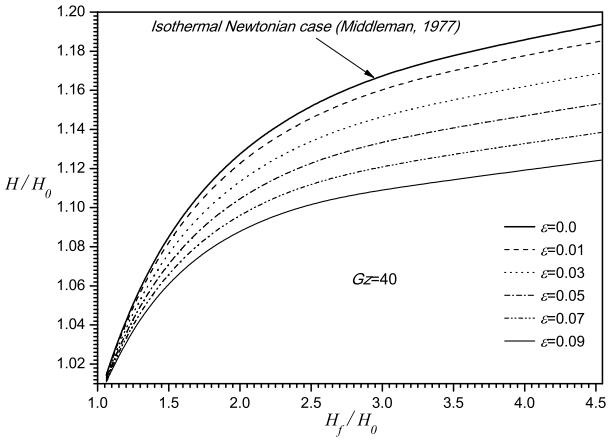

Figure 7: The dimensionless exiting sheet thickness H/H_0 as a function of the entering sheet thickness H_f/H_0 for different values of the parameter ε, for a Newtonian fluid with Gz =40.

H/H_0, as a function of the dimensionless entering sheet thickness, H_f/H_0, under the influence of the parameters ϵ, for Gz =40. In order to determine the correction λ_1 because of thermal effects, the Eq. (53) was solved iteratively as a function of λ_0, θ_0 and u_0. The obtained results for λ_0 and λ_1 are replaced in the expansion of λ, given by $\lambda = \lambda_0 + \epsilon\lambda_1 + \cdots$, for different values of the parameter ϵ. In this work we have assumed that the rolls were fed with a sheet of fluid with finite thickness, as suggested in Fig. 1; in this case the dimensionless entering sheet thickness H_f/H_0 is a known parameter as it is shown in Fig. 2. In this figure, for a fixed value of H_f/H_0, the leave-off distance and the exiting sheet thickness decreases as the parameter ϵ increases, it is evident that non-isothermal Newtonian case produces thinner sheets than the isothermal Newtonian fluid. With the parametric values shown in Figs. 7. For H_f/H_0 =4.54 and ϵ =0.09, the exiting sheet thickness is reduced in a 6 %, compared with the Newtonian isothermal case.

5 CONCLUSIONS

In this paper, we have studied theoretically the influence of the viscous dissipation and temperature-dependent consistency index on the exiting sheet thickness, for a Newtonian fluid flowing between two cylinders rotating at the same velocity and temperature. The solution is

based on the regular perturbation technique and the resulting governing equations are based on the well-known Lubrication theory. The numerical results predict the dimensionless velocity field, pressure, temperature distribution, and the exit locations and the exiting sheet thickness corrected by thermal effects. *A variation of 5.89 percent in the dimensionless exiting sheet thickness was determined*. As it has been shown, in the limit of $\epsilon \to 0$, the present solution smoothly approaches the unperturbed or zeroth-order solution, which correspond to the isothermal case reported by Middleman (1977).

ACKNOWLEDGEMENTS

This work has been supported by the research grants no. 58817 of Consejo Nacional de Ciencia y Tecnología (CONACYT) at Mexico.

REFERENCES

Bird R.B., Armstrong R.C., and Hassager O. *Dynamics of Polymeric Liquids, Vol 1 Fluid Mechanics*. John Wiley & Sons, Canada, 1987.

C. Kiparissides J.V. A study of viscous dissipation in the calendering of power-law fluids. *Polymer Engineering and Science*, 18(3):210–214, 1978.

Dantzig J.A. and Tucker C.L. *Modeling in Materials Processing*. Addison-Wesley, Cambridge University Press, 2001.

Dobbels F. and Mewis J. Nonisothermal nip flow in calendering operation. *AIChE Journal*, 23(3):224–232, 1977.

Gaskell R.E. The calendering of plastic materials. *Journal of Applied Mechanics*, 17:334–337, 1950.

Hoffman J.D. *Numerical Methods for Engineers and Scientist*. CRC Press, New York, 2001.

Mckelvey J.M. *Polymer Processing*. Wiley, New York, 1962.

Middleman S. *Fundamentals of Polymer Processing*. McGraw-Hill, United States of America, 1977.

Mitsoulis E. Numerical simulation of calendering viscoplastic fluids. *Journal of Non-Newtonian Fluid Mechanics*, 154:77–88, 2008.

Osswald T. and Ortiz J.P.H. *Polymer Processing*. Carl Hanser Verlag, Munich, 2006.

Pearson J.R. *Mechanical Principles of Polymer Melt Processing*. Pergamon Press, London, 1966.

Sofou S. and Mitsoulis E. Calendering of pseudoplastic and viscoplastic sheets of finite thickness. *Journal of Plastic Film & Sheeting*, 20:185–222, 2004.

Tadmor Z. and Gogos C.G. *Principles of Polymer Processing*. John Wiley & Sons, Haifa, Israel, 1979.

Wendt J.F. *Computational Fluid Dynamics*. Springer, 2009.

Zheng R. and Tanner R.I. A numerical analysis of calendering. *Journal of Non-Newtonian Fluid Mechanics*, 28:149–170, 1988.